Signature of the Charged Higgs Decay $H^{\pm} \rightarrow Wh^0$ With the ATLAS Detector

Kétévi Adiklè Assamagan
Hampton University, Hampton, VA 23668 USA

Abstract

The possibility of detecting the charged Higgs through the process $H^{\pm} \rightarrow Wh^0$ is studied with the ATLAS detector. Good reconstruction of the charged Higgs mass is achieved for masses below and above the top-quark mass and the $t\bar{t}$ background can be suppressed substantially. However, because the signal rates are low, the discovery potential of this channel is limited to a rather narrow area of MSSM parameter space. The results can be applied to other models, for instance, NMSSM where the discovery potential could extend to a significant area of the parameter space.

1 Introduction

The Higgs sector of the Minimal Supersymmetric Standard Model (MSSM) contains five physical states, two of which are charged, $H^{\pm}$, and the other three are neutral (h^0, H^0, and A^0) [1]. Thus far, the study of the discovery potential of the charged Higgs with ATLAS has concentrated mainly on the fermionic decays modes — $H^{\pm} \rightarrow tb$ and $H^{\pm} \rightarrow \tau\nu$ are the dominant decay channels in most of the parameter space [2]. In the present paper, the discovery potential of the charged Higgs with the ATLAS detector through the process $H^{\pm} \rightarrow Wh^0$ is studied. Though significant only in a tiny range of MSSM parameter space [3], this channel constitutes a unique test for MSSM and is also sensitive to the next-to-minimal extension to MSSM, i.e., NMSSM, where there may be a significant range of viability below and above the top-quark mass [4]: NMSSM extends the Higgs sector of MSSM by adding a complex singlet scalar field. The parameter space is therefore less constrained than that of MSSM and as a result, the indirect lower limits on the Higgs masses from LEP are no longer valid [4]. In addition, the mixing between the singlet and the doublet states would dilute the direct mass limits on the latter from LEP.

The present study is carried out in the framework of PYTHIA5.7 [5] and ATLFAST [6]. In the following sections, the details of the analysis are presented.

2 $H^{\pm} \rightarrow W^*h^0$, $m_{H^{\pm}} < m_t$

Below the top-quark mass, we consider $t\bar{t}$ production with one top-quark decaying into W and the other into the charged Higgs. In this case, the W from the charged Higgs decay is off mass shell. The characteristics of the production and decay

processes are:

$$gg\,(q\bar{q}) \;\to\; t\bar{t} \tag{1}$$

$$t \;\to\; H^{\pm}\,b \tag{2}$$

$$\bar{t} \;\to\; W\,\bar{b} \tag{3}$$

$$H^{\pm} \;\to\; W^{*}\,h^{0}. \tag{4}$$

Thus, the spectrum contains two W's, one of which is off mass shell, and four b-quarks due to the subsequent decay $h^0 \to b\bar{b}$. In the present analysis, one of the W's is required to decay into leptons (e, μ), and the other into jets. The major background of this process comes from $t\bar{t}b\bar{b}$ and $t\bar{t}q\bar{q}$ production where both top-quarks decay into W's. Table 1 summarizes the estimated rates for signal and background as a function of $\tan\beta$ and $m_{H^{\pm}}$. The results presented in this paper

Table 1: The expected rates ($\sigma \times BR$), for the signal $t\bar{t} \to bH^{\pm}Wb$ with $H^{\pm} \to W^{*}h^{0}$, and the $t\bar{t}$ backgrounds. It should be noted that due to the $\tan\beta$ dependence of the $t \to H^{\pm}b$ and of the $t \to Wb$ branching ratios, the $t\bar{t}$ background rates depend on $\tan\beta$.

Process	$\tan\beta$	m_{h^0} (GeV)	$m_{H^{\pm}}$ (GeV)	$\sigma \times$ BR (pb)
$H^{\pm} \to W^{*}\,h^{0}$	2.0	83.5	152	1.2
	3.0	93.1	152	0.2
$t\bar{t} \to jjbl\nu b$	2.0			143
	3.0			152

correspond to the high luminosity operation, with an integrated luminosity of 300 fb^{-1}. A lepton identification efficiency of 90% and a b-tagging efficiency of 50% are assumed. A value of the charged Higgs mass smaller than that shown in Table 1 results in smaller signal rate as the branching ratio for $H^{\pm} \to Wh^{0}$ drops very rapidly. On the other hand, when $m_{H^{\pm}}$ is closer to the top mass, one of the four b-quarks (mainly the b-quark from $t \to H^{\pm}b$) becomes too soft (to be

identified and tagged as a b-jet). In this case, good efficiency for the signal can be achieved by requiring three b-tagged jets but with this requirement, it is more difficult to effectively suppress the background. Although the signal acceptance drops by a factor of two if a fourth b-tagged jet is required, the background is suppressed by a factor of twenty-five such that the final signal significance can be increased. The following algorithm is used to select signal events:

2-a Search for one isolated lepton (e or μ with $p_T^e > 20$ or $p_T^\mu > 6$ GeV and $|\eta| < 2.5$), four b-tagged jets (with $p_T^b > 30$ GeV and $|\eta| < 2.5$), and at least 2 non b-jets with $p_T^j > 30$ GeV.

2-b Two possible scenarios are considered on an event by event basis:

$$W^* \to l\nu \qquad W \to jj \tag{5}$$

or

$$W^* \to jj \qquad W \to l\nu. \tag{6}$$

If the on-shell W decays into leptons, then the W mass constraint is used to fix the longitudinal component p_L^ν of the neutrino momentum. This leads, in general, to two solutions. If no physical solution is found, the event is rejected. For this case, $W^* \to jj$ and all the jet-jet combinations retained in **2-a** are accepted. However, if $W^* \to l\nu$ instead, one can no longer use the W mass constraint. In this case, p_L^ν is set to zero and the jet-jet combinations consistent with the W-mass are retained, i.e., $|m_W - m_{jj}| < 25$ GeV; in this mass window, the jet momenta are rescaled so that

$$m_{jj} = m_W \tag{7}$$

before proceeding further. Such a relatively wide W-mass window cut provides a better acceptance on final selections.

2-c For both scenarios described in **2-b**, consider all the combinations $t_{Wb} \to Wb_i$, $h^0 \to b_j b_k$, $H^{\pm} \to h^0 W^*$ and $t_{H^{\pm}b_l} \to H^{\pm}b_l$ and retain that combination which minimizes

$$\chi^2 = (m_{Wb_i} - m_t)^2 + (m_{H^{\pm}b_l} - m_t)^2 + (m_{b_j b_k} - m_{h^0})^2. \qquad (8)$$

Figure 1 shows the mass reconstructions for the W's as obtained from **2-b** and for both top-quarks from the optimization procedure, **2-c**. Tracing back to the parton level information from PYTHIA outputs, it is estimated that the chi-square criterion (Equation 8) selects the correct combinations of both top-quarks and the neutral light Higgs in 41% of the cases. The $m_{H^{\pm}b}$ distributions for the correct matchings, and as a result of the optimization procedure are shown in Figure 2.

2-d Reconstruct $m_{W^*b_l}$: the signal channel $t_{H^{\pm}b_l} \to W^*h^0b_l$ is replaced in the background by $t \to Wb_l$: one would expect $m_{W^*b_l}$ to be consistent with the top mass for the background but not for the signal. Thus, we retain the event if the following condition is satisfied:

$$|m_{Wb_i} - m_t| < 25 \quad \text{and} \quad |m_{W^*b_l} - m_t| > 50 \text{ GeV}. \qquad (9)$$

2-e Select events where $t \to H^{\pm}b_l$ is reconstructed in the 50 GeV mass window, $|<m_{H^{\pm}b_l}> - m_t| < 50$ GeV, and $h^0 \to b_j b_k$ within a mass window of 25 GeV, $|<m_{b_j b_k}> - m_{h^0}| < 25$ GeV. The charged Higgs mass reconstruction following this cut is shown in Figure 3.

Table 2 shows the efficiency of the cuts **2-a** through **2-e** for the signal and for the background. The expected significances and signal-to-background ratios are shown in Table 3 for $\tan\beta = 2$ and for $\tan\beta = 3$, and for an integrated luminosity of 300 fb^{-1}. This channel presents a significant discovery potential at low

Table 2: Efficiencies of the cuts **2-a**, **2-b**, **2-c**, **2-d** and **2-e** for the signal and the background, shown from the third column. Also shown is the successive improvement in the signal-to-background ratio as a result of the cuts. The significances and the signal-to-background ratios shown in Table 3 are calculated within $\pm 2\sigma_{H^{\pm}}$ of $<m_{H^{\pm}}>$.

Process	$\tan\beta$	**2-a**	**2-b**	**2-c**	**2-d**	**2-e**
Signal (%)	2.0	2.5	2.1	2.1	1.0	0.7
Background (%)		0.09	0.07	0.07	0.02	$2.0\,10^{-3}$
S:B		1:5	1:4	1:4	1:3	2.9:1
Signal (%)	3.0	2.7	2.3	2.3	1.1	0.8
Background (%)		0.10	0.07	0.07	0.02	$2.1\,10^{-3}$
S:B		1:28	1:23	1:20	1:10	1:2.0

$\tan\beta$ (< 2.5) as seen from Figure 3 and Table 3. At high $\tan\beta$, the reconstruction procedure works also well in suppressing the background significantly. From Table 1, for $\tan\beta = 2$, the signal-to-background ratio is below 1:100 at the start. The improvement in the suppression of the background is also shown in Table 2; for instance, at $\tan\beta = 2$, the signal-to-background ratio improves to 2.9:1 after all cuts. The difficulty in extracting an observable signal at high $\tan\beta$ is due mainly to the low signal rate: in fact, as seen in Table 1, the signal rate drops by the factor of six from $\tan\beta = 2$ to $\tan\beta = 3$ while the background remains approximately the same. It should be noted that in Table 2, the significances and the signal-to-background ratios are calculated taking all the events satisfying the respective cuts. In Table 3, the same quantities are calculated within $\pm 2\sigma_{H^{\pm}}$ of $<m_{H^{\pm}}>$, after all cuts. This explains the improvement shown in Table 3 over the last column of Table 2.

In summary, the discovery potential of the charged Higgs through the decay $H^{\pm} \to W^{*}h^{0}$ for $m_{H^{\pm}} < m_t$ has been studied. Although the signal rate is initially two orders of magnitude smaller than the $t\bar{t}$ background rate, the proposed

Table 3: The expected signal-to-background ratios and significances for an integrated luminosity of 300 fb^{-1}. $<m_t>$, $<m_{H^{\pm}}>$ and $<m_{h^0}>$ are the means of the Gaussian fits to the distributions of $m_{H^{\pm}b}$, $m_{W^{*}h^0}$ and $m_{b\bar{b}}$ respectively. The nominal values are shown in Table 1 for $m_{H^{\pm}}$ and m_{h^0}. A central value of 175 GeV is taken for the top-quark mass. $m_{H^{\pm}}$ and m_t are not reconstructed at their nominal values (within the large statistical uncertainties, the numbers are consistent with the nominal values): this is due to the assumption that $p_L^{\nu} = 0$ (made in **2-b**) and also to the fact that the 4-momentum of the W^* in $H^{\pm} \to W^{*}h^{0}$ and $t \to W^{*}h^{0}b$ is not rescaled to the W mass before reconstructing the charged Higgs and the top-quark. As seen from Figure 1, the other top-quark is reconstructed to the nominal value since here, $t \to Wb$; this W is on-shell: in the leptonic channel the W mass constraint guarantees that $m_{l\nu} = m_W$, and in the hadronic channel, the jet momenta are rescaled within a mass window according to Equation 7. The significances and the signal-to-background ratios are calculated within $\pm 2\sigma_{H^{\pm}}$ of $<m_{H^{\pm}}>$. This explains the improvement over the results shown in the last column of Table 2.

	$\tan\beta = 2$	$\tan\beta = 3$
$<m_t>$ (GeV)	188 ± 20	190 ± 29
σ_t (GeV)	18 ± 11	20 ± 10
$<m_{H^{\pm}}>$ (GeV)	157 ± 7	160 ± 10
$\sigma_{H^{\pm}}$ (GeV)	19 ± 8	21 ± 10
$<m_{h^0}>$ (GeV)	83 ± 1	92 ± 4
σ_{h^0} (GeV)	12 ± 1	13 ± 3
Signal events	136	25
Background events	40	43
S/B	3.4	0.6
$S/\sqrt{B}$	21.5	3.8

reconstruction procedure permits the extraction of the signal with a significance exceeding 5σ in the low $\tan\beta$ $(1.5-2.5)$ region. At high $\tan\beta$, though the reconstruction efficiency remains comparable, the signal rate decreases so significantly that the discovery potential vanishes in this region.

3 $H^{\pm} \to Wh^0, m_{H^{\pm}} > m_t$

Above the top-quark mass, the charged Higgs is produced in association with a top-quark according to:

$$gb \to tH^{\pm} \quad (10)$$

$$H^{\pm} \to Wh^0 \quad (11)$$

$$t \to Wb. \quad (12)$$

The final state for the signal contains two W's, one of which is required to decay into leptons (electron or a muon to trigger the experiment), the other into jets, and three b-jets due to the subsequent decay $h^0 \to b\bar{b}$. The background in this case comes from $t\bar{t}b$ and $t\bar{t}q$ events with both top-quarks decaying into W's. Table 4 shows the signal and the background rates as a function of $\tan\beta$. The

Table 4: The rates for the signal $bg \to H^{\pm}t \to Wh^0\,Wb$ and the $t\bar{t}$ background as a function of $\tan\beta$.

Process	$\tan\beta$	m_{h^0} (GeV)	$m_{H^{\pm}}$ (GeV)	$\sigma \times$ BR (pb)
$H^{\pm} \to W\,h^0$	1.5	78.0	250	0.023
	3.0	99.1	200	0.134
	5.0	104.9	200	0.031
$t\bar{t} \to jjbl\nu b$				228

same kinematic cuts on η and p_T, and the same efficiencies as in the case $m_{H^{\pm}} < m_t$ are assumed. The analysis procedure is described below:

3-a Search for one isolated lepton (e or μ), three b-tagged jets, and at least two non b-jets satisfying the kinematic conditions stated in **2-a**.

3-b In this case, both W's are on-shell and the W mass constraint is used to find a longitudinal component of the neutrino momentum. If no physical solution is found, the event is rejected.

3-c Retain all the jet-jet combinations consistent with the W mass, i.e., $|m_{jj} - m_W| < 25$ GeV, and within this mass window, the jet momenta are rescaled to give $m_{jj} = m_W$ before proceeding further.

3-d All the $l\nu\, b$ and jjb combinations are considered and the associated top-quark from $gb \to tH^{\pm}$, $t \to W_i b_k$ and the neutral light Higgs, $h^0 \to b_l b_m$, are reconstructed by minimizing the chi-square

$$\chi^2 = (m_{W_i b_k} - m_t)^2 + (m_{b_l b_m} - m_{h^0})^2. \tag{13}$$

Figure 4 shows the reconstructions of the W's, the associated top, and of the neutral light Higgs boson. This procedure not only reconstructs the associated top and the neutral Higgs but it also establishes whether the W_i selected in the minimization comes from **3-b** or **3-c**. By comparing with parton level information, the purity of the reconstructions of the associated top-quark and of the neutral Higgs is found to be 50%. The reconstruction of the charged Higgs itself is not unique: if the optimization procedure selects a W_i from the leptonic channel, $t \to W_i b_k \to l\nu b_k$, there are still as many charged Higgs candidates as the number of jet-jet combinations retained in **3-c**: $H^{\pm} \to W_j h^0 \to jjb_l b_m$. On the other hand, if the optimization procedure selects a W_i from the hadronic channel, $t \to W_i b_k \to jjb_k$, there are, in general, two charged Higgs candidates as a result of the quadratic ambiguity in the calculation of the longitudinal component p_L^{ν} of the neutrino momentum from **3-b**: $H^{\pm} \to W_j h^0 \to l\nu b_l b_m$. The event is accepted for further processing if

$$|m_{W_i b_k} - m_t| < 25 \text{ GeV}$$

and

$$|m_{b_l b_m} - m_{h^0}| < 25 \text{ GeV}, \tag{14}$$

and the momenta of the b-jets from $h^0 \to b\bar{b}$ are rescaled so that $m_{b\bar{b}} = m_{h^0}$ before reconstructing $H^{\pm}$. Figure 5 shows the mass reconstructions for the charged Higgs, $H^{\pm} \to W h^0$. It is possible to improve the signal reconstruction by making cuts on $p_T^{H^{\pm}}$, $\Delta R_{h^0 W}$, $p_T^{b_l b_m}$ and $\Delta R_{b_l b_m}$ as shown in the bottom plots of Figure 5.

Table 5: Efficiencies of the cuts **3-a**, **3-b**, **3-c** and **3-d** for the signal and the background, shown from the third column.

Process	$\tan\beta$	**3-a**	**3-b**	**3-c**	**3-d**
Signal (%)	1.5	18	13	13	6
	3.0	17	12	12	6
Background (%)		3.3	2.3	2.3	0.6

The efficiencies of the cuts **3-a** through **3-d** for the signal and the background are shown in Table 5. For an integrated luminosity of 300 fb^{-1}, Table 6 shows

Table 6: The expected signal-to-background ratios and the significances (calculated within $\pm 2\sigma_{H^{\pm}}$ of $<m_{H^{\pm}}>$) for an integrated luminosity of 300 fb^{-1}. $<m_{H^{\pm}}>$ and $<m_{h^0}>$ are the means of Gaussian fits to the distributions of m_{Wh^0} and $m_{b\bar{b}}$ respectively. The nominal values are shown in Table 4.

	$\tan\beta = 1.5$, $m_A = 237$ GeV	$\tan\beta = 3$, $m_A = 184$ GeV
$<m_{H^{\pm}}>$ (GeV)	252	202
$\sigma_{H^{\pm}}$ (GeV)	22	13
$<m_{h^0}>$ (GeV)	80	101
σ_{h^0} (GeV)	12	15
Signal events	58	236
Background events	7687	5000
S/B	0.008	0.05
$S/\sqrt{B}$	0.7	3.3

the expected signal-to-background ratios and the significances at $\tan\beta = 1.5$ and

3. This channel does not present any discovery potential for the charged Higgs. This is due the to the low signal rate at the start (see Table 4); the ratio of the signal to background is S:B=1:1700 ($\tan\beta = 3$) before any cut is applied. The series of cuts **3-a** to **3-d** improves this ratio to S:B=1:20 for $\tan\beta = 3$ as shown in Table 6. However, the ultimate significance is only 3.3 after three years of running at high luminosity. It is possible to reduce the number of charged Higgs candidates resulting from **3-d**, $H^{\pm} \rightarrow W_j b_l b_m$ by reconstructing the invariant masses $m_{W_j b_l}$ and $m_{W_j b_m}$ and demanding that the latter not be consistent with the top-quark mass, i.e.,

$$|m_{W_j b_l} - m_t| > 25 \text{ GeV}$$

and

$$|m_{W_j b_m} - m_t| > 25 \text{ GeV}$$

This additional requirement does not improve the reconstruction significantly.

4 Conclusions

The possibility of detecting the charged Higgs through the decay $H^{\pm} \rightarrow Wh^0$ with the ATLAS detector has been studied. Below the top-quark mass, $t\bar{t}$ production is the dominant production mechanism, with one of the top-quarks decaying into the charged Higgs, $t \rightarrow H^{\pm}b$. The W from the subsequent decay of $H^{\pm}$ is off-shell, $H^{\pm} \rightarrow W^*h^0$. The final state signature contains an isolated lepton, four b-tagged jets and at least two non b-jets. This requirement suppresses quite significantly the $t\bar{t}b\bar{b}$ and $t\bar{t}q\bar{q}$ backgrounds. In fact, although initially the backgrounds are two orders of magnitude higher than the signal, the reconstruction technique presented here allows for a significant discovery potential in the low $\tan\beta$ region (1.5-2.5). At higher $\tan\beta$, the reconstruction efficiency remains comparable but

the signal rates are too low.

Above the top-quark mass, the charged Higgs is produced in association with a top-quark, $gb \rightarrow tH^{\pm}$. In this case, the search for a final state with an isolated lepton, three b-tagged jets and at least two non b-jets has been performed. Initially, the total background is at least three orders of magnitude higher than the signal in the most favorable case ($\tan\beta = 3$). However, with the reconstruction technique presented here, the signal-to-background ratios could be improved by two orders of magnitude. This improvement is still insufficient to observe the signal over the background; for example, at $\tan\beta = 3$, a significance of only 3.3 can be expected after 3 years at high luminosity.

In MSSM, the $H^{\pm} \rightarrow Wh^0$ channel has been excluded by LEP-2 up to $\tan\beta = 3$ because of the non-observation of h^0 [4] [7]. Beyond $\tan\beta = 3$, as demonstrated by the study shown here, this channel presents no discovery potential due to the very low signal rate. It has been argued that in the singlet extension to MSSM, i.e., NMSSM, this channel is immune to the LEP constraints and there may be a significant discovery potential above and below the top-quark mass [4]. This underscores the main objective of the present study, which is to demonstrate a good signal reconstruction and a high background suppression with the ATLAS detector. The result shown can be normalized to models other than MSSM, for instance NMSSM.

Acknowledgements

The author expresses immense gratitude to E. Richter-Wąs for fruitful discussions and constructive criticisms. The present work is supported by a grant from the USA National Science Foundation (grant number 9722827).

References

[1] P. H. Nilles, *Phys. Rev.* **110**, 1 (1984); H. Haber and G. Kane, *Phys. Rev.* **115**, 75 (1985).

[2] D.H. Miller, S. Moretti, D.P. Roy, and W.J. Stirling, hep-ph/9906230; S. Moretti and D.P. Roy, hep-ph/9909435; K.A. Assamagan, ATLAS Note ATL-PHYS-99-013.

[3] S. Moretti and W.J. Sterling, *Phys. Lett.* **B347** (1995) 291; Erratum, ibidem **B366** (1996) 451.

[4] M. Dress, M. Guchait and D.P. Roy, hep-ph/9909266; and the references therein.

[5] T. Sjöstrand, "High-Energy Physics Event Generation with PYTHIA 5.7 and JETSET 7.4", CERN preprints-TH.7111/93 and CERN-TH.7112/93, Comp. Phys. Comm. **82** (1994) 74.

[6] E. Richter-Wąs, D. Froidevaux and L. Poggioli, ATLAS Internal Note, PHYS-No-079 (1996).

[7] R. Barate, ALEPH Collaboration, *Phys. Lett.* **B440**, (1998) 419.

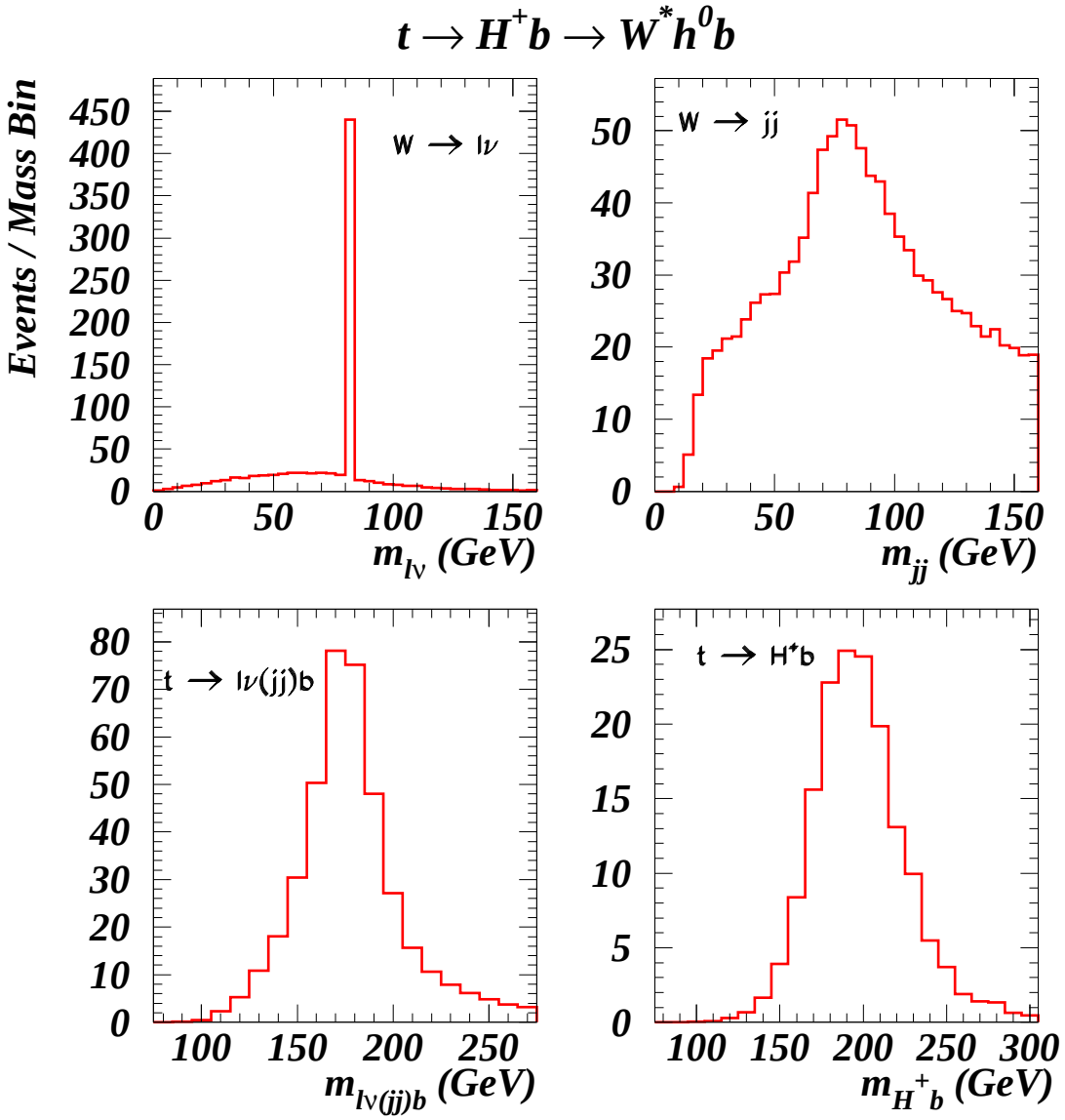

Figure 1: The mass reconstructions for the W's and the top-quarks. The data is shown for the signal only and for an integrated luminosity of 300 fb^{-1}. The top left plot shows a spike at 80 GeV corresponding to $W \to l\nu$ and a broad distribution coming from $W^* \to l\nu$. $t \to Wb$ is reconstructed at the nominal value of $m_t = 175$ GeV as seen from the bottom left plot. However, $t \to H^{\pm} b \to W^* h^0 b$ is not reconstructed to the nominal value of m_t; this is due to the assumption that $p_L^{\nu} = 0$ (made in **2-b**) and also to the fact that the 4-momentum of W^* is not rescaled to the W-mass before the reconstruction of $H^{\pm} \to W^* h^0$ and of $t \to H^{\pm} b$.

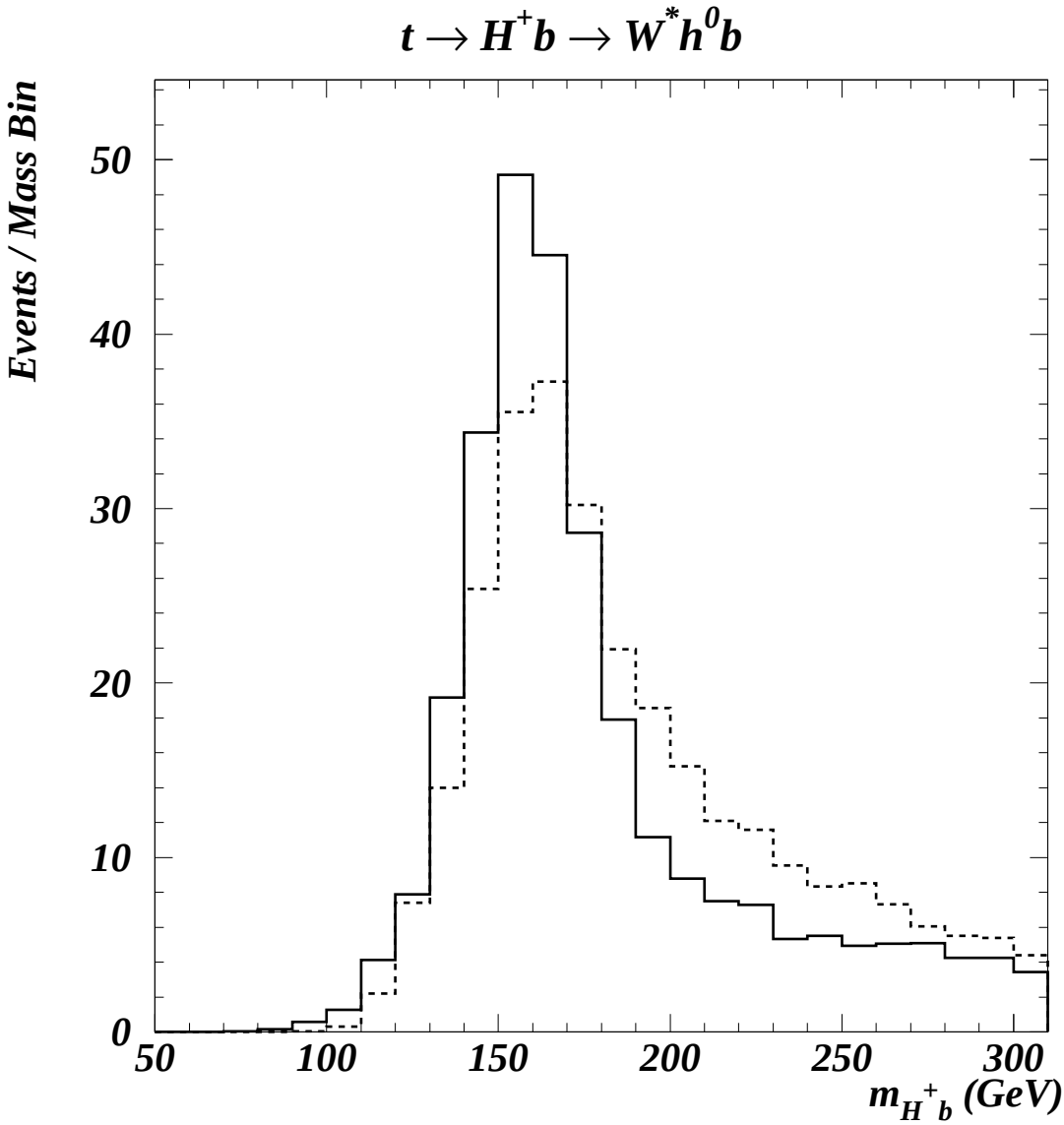

Figure 2: The $m_{H^\pm}$ distributions from correct matchings (solid line), and as obtained from the optimization procedure (dashed line). It has been estimated that in 41% of the cases, the selection criteria reconstruct correctly both top-quarks and the neutral light Higgs.

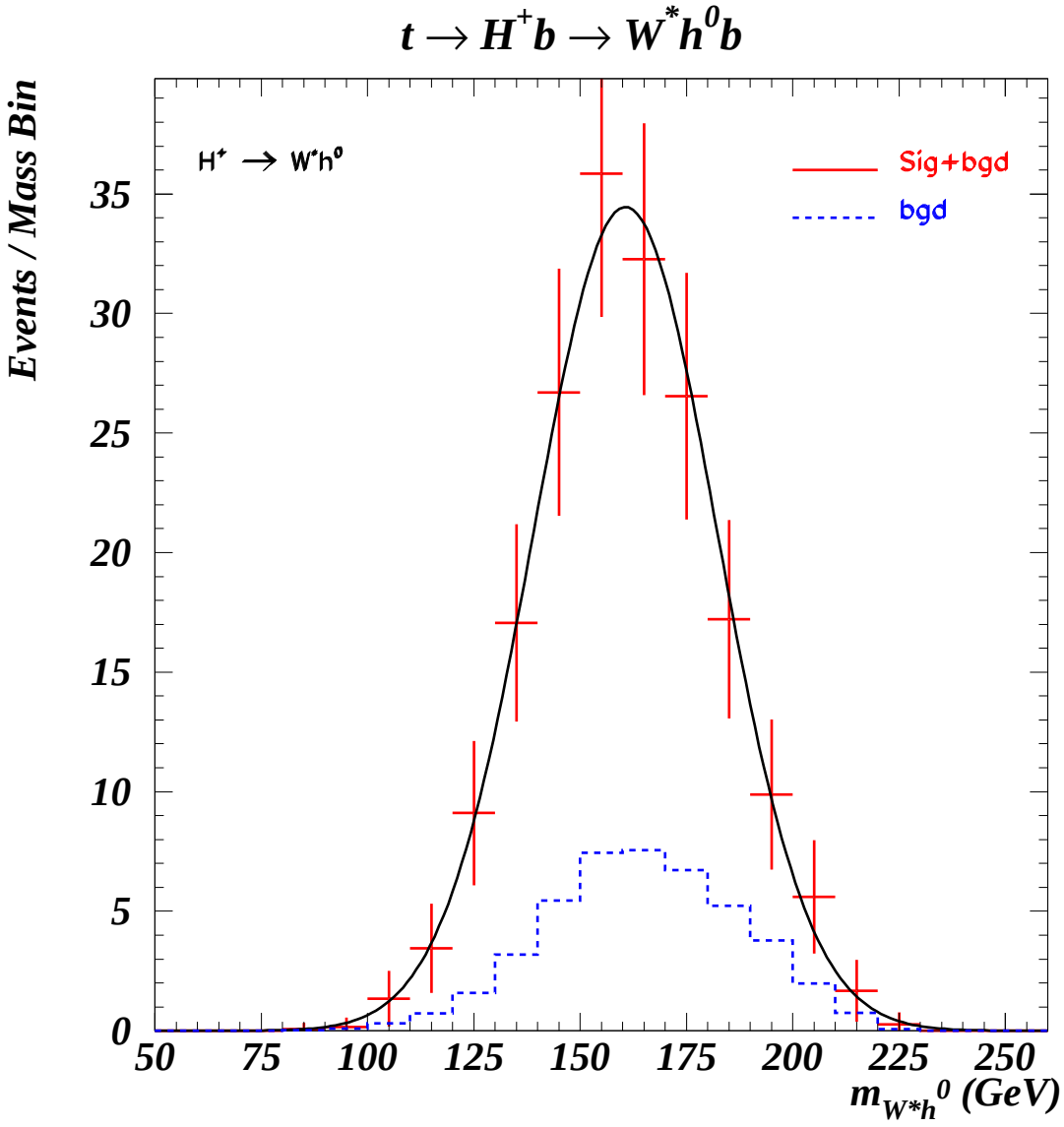

Figure 3: The final mass reconstruction for the charged Higgs for $\tan\beta = 2$ after cut **(e)** is applied. The results shown in Table 3 are obtained from this data. A significant discovery potential for this channel is expected in the low $\tan\beta$ region $(1.5 - 2.5)$. At higher $\tan\beta$, the signal rate decreases so much that the discovery potential vanishes.

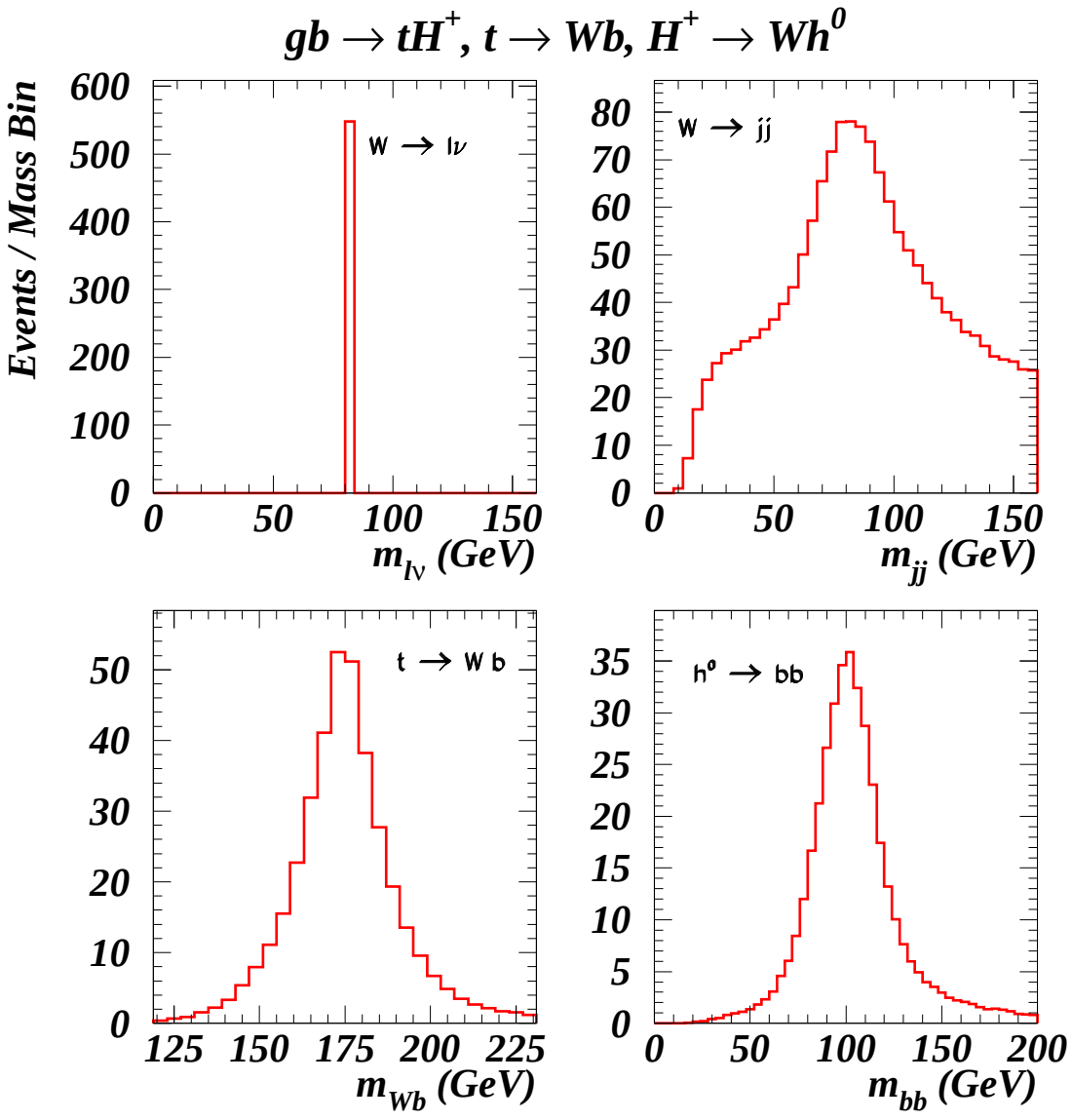

Figure 4: The mass reconstructions for the W's, the associated top, and for the neutral light Higgs for $\tan\beta = 3$ and for an integrated luminosity of 300 fb^{-1}. Only the signal is shown. Both the top-quark and the neutral Higgs masses are reconstructed at their nominal values.

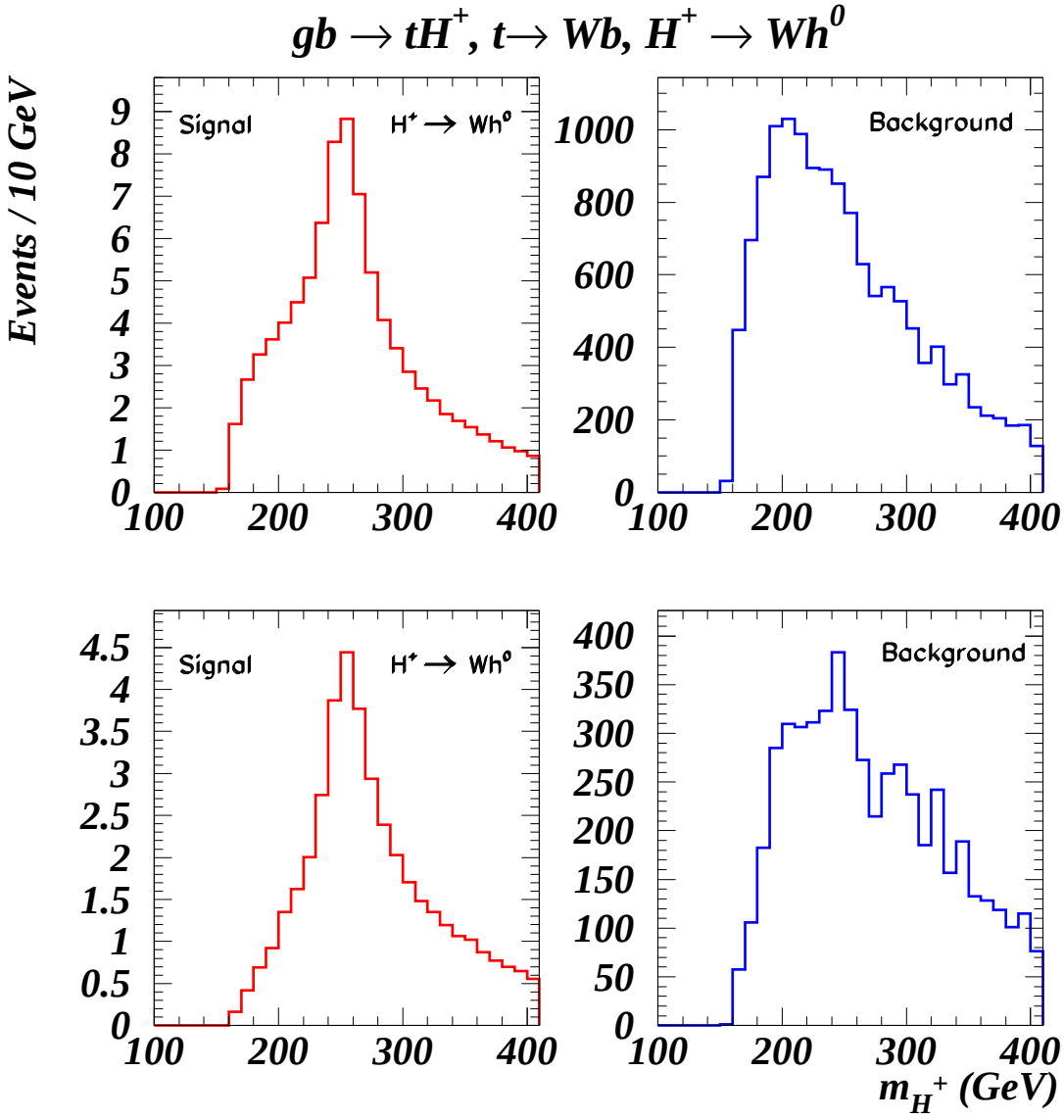

Figure 5: The mass reconstructions for the charged Higgs after all cuts, **3-d**, for $m_{H^\pm} = 250$ GeV, $\tan\beta = 1.5$, and for an integrated luminosity of 300 fb^{-1}. The results of Table 6 are obtained from this data (top plots). The bottom plots correspond to reconstructions after additional kinematic cuts: $p_T^{H^\pm} > 30$ GeV, $2 < \Delta R_{Wh^0} < 4$, $p_T^{h^0} > 30$ GeV and $0.5 < \Delta R_{b\bar{b}} < 2$. These cuts do not improve much the overall significance of the signal although the signal resolution improves by 15%.